[7] Kaplun, S., "The Role of Coordinate Systems in Boundary-Layer Theory," *Zeitschrift für Angewendte Matematik und Physik*, Vol. 5, 1954, pp. 111–135.

[8] Cheng, H. K., "The Blunt-Body Problem in Hypersonic Flow at Low Reynolds Number," Rept. AF-1284-A-10, 1963, Cornell Aero Lab., Ithaca, New York.

[9] Davis, R. T., "Numerical Solution of the Hypersonic Viscous Shock-Layer Equations," *AIAA Journal*, Vol. 8, No. 5, May 1970, pp. 843–851.

[10] Cheng, H. K., Chen, S. H., Mobley, R., and Huber C. R., "The Viscous Hypersonic Slender-Body Problem: A Numerical Approach Based on a System of Composite Equations," Rept. RM-6193-PR, 1970, Rand Corp., Santa Monica, Calif.

[11] Douglas, J., "On the Numerical Integration of $\partial^2 u/\partial x^2 + \partial^2 u/\partial y^2 = \partial u/\partial t$ by Implicit Methods," *Journal of the Society for Industrial and Applied Mathematics*, Vol. 3, pp. 42–65.

[12] Davis, R. T., "Numerical Solution of the Navier-Stokes Equations for Symmetric Laminar Incompressible Flow Past a Parabola," *Journal of Fluid Mechanics*, Vol. 51, Part 3, Feb. 1972.

[13] Wilkinson, J., "A Note on the Oseen Approximation for a Paraboloid in a Uniform Stream Parallel to its Axis," *Quarterly Journal of Mechanics and Applied Mathematics*, Vol. 8, 1955, pp. 415–421.

[14] Mark, R. M., "Laminar Boundary-Layers on Slender Bodies of Revolution in Axial Flow," Rept. 21, 1954, Guggenheim Aeronautical Lab., California Inst. of Technology, Pasadena, Calif.

[15] Mather, D. J., "The Motion of Viscous Liquid Past a Paraboloid," *Quarterly Journal of Mechanics and Applied Mathematics*, Vol. XIV, Pt. 4, 1961, pp. 423-429.

[16] Albacete, L. M., "Boundary-Layer Over a Slender Parabola of Revolution with Fluid Injection," *AIAA Journal*, Vol. 4, No. 11, Nov. 1966, pp. 2040–2041.

[17] Lee, L. L., "Boundary-Layer Over a Thin Needle," *The Physics of Fluids*, Vol. 10, No. 4, April 1967, pp. 820–822.

[18] Cebeci, T., Na, T. Y. and Mosinskis, G., "Laminar Boundary-Layers on Slender Paraboloids," *AIAA Journal*, Vol. 7, No. 7, July 1969, pp. 1372–1374.

[19] Miller, D. R., "The Boundary-Layer on a Paraboloid of Revolution," *Proceedings of the Cambridge Philosophical Society*, Vol. 65, 1969, pp. 285-298.

[20] Van Dyke, M., "Flow Past a Parabola at Low Reynolds Number," *Journal of Fluid Mechanics*, 1972, to be published.

[21] Thomas, L. H., "Elliptic Problems in Linear Difference Equations Over a Network," Rept., 1949, Watson Science Computing Lab., Columbia University, New York.

[22] van de Vooren, A. I. and Dijkstra, D., "The Navier-Stokes Solution for Laminar Flow Past a Semi-Infinite Flat Plate," *Journal of Engineering Mathematics*, Vol. 4, 1970, pp. 9–27.

[23] Veldman, A. E. P. and Dijkstra, D., "The Numerical Solution of the Navier-Stokes Equations for Laminar Flow Past a Parabolic Cylinder," Rept. TW-93, 1971, Mathematisch Instituut Rijksuniversiteit Groningen.

[24] Davis, R. T., "Laminar Incompressible Flow Past the Parabola and the Paraboloid," *Proceedings of the 12th International Congress of Applied Mechanics*, 1968.

[25] Davis, R. T., "Boundary-Layers on Parabolas and Paraboloids by Methods of Local Truncation," *International Journal of Non-Linear Mechanics*, Vol. 4, 1970, pp. 625-632.

SEPTEMBER 1972 AIAA JOURNAL VOL. 10, NO. 9

Nonsimilar Solution for Laminar and Turbulent Boundary-Layer Flows over Ablating Surfaces

ROBERT M. KENDALL* AND LARRY W. ANDERSON†
Aerotherm Corporation, Mountain View, Calif.
AND
RONALD H. AUNGIER‡
Air Force Weapons Lab, Kirtland Air Force Base, N. Mex.

A mathematical model and numerical solution of nonsimilar laminar or turbulent multicomponent chemically reacting boundary-layer flows are presented. The general flow model and solution technique represent an extension of a previously presented laminar flow scheme to the turbulent regime and to a broader set of boundary conditions. The turbulent model, which includes a mixing length representation in the wall region and a constant eddy viscosity in the wake region, represents a compressible flow adaption of a previously validated incompressible turbulent model. Boundary conditions for the solution procedure include features which are most useful for re-entry calculations with ablation, such as direct coupling with an entropy layer, with an ablating wall or with surface injection. Sample problems have been selected which illustrate these features, demonstrate the necessity for a nonsimilar analysis, and validate the compressible flow turbulent model.

Nomenclature

c_t = thermal diffusion constant (Ref. 4)
C = density-viscosity product normalized by reference values
$\bar{C}_p$ = frozen specific heat of the gas mixture
$\tilde{C}_p$ = gas mixture property which reduces to $\bar{C}_p$ when all diffusion coefficients are equal (Ref. 4)
C_{p_i} = specific heat of species i
$\bar{D}$ = reference binary diffsion coefficient of Ref. 6
D_i^T = multicomponent thermal diffusion coefficient for species i
D_{ij} = multicomponent diffsion coefficient for species i and j
$\mathscr{D}$ = diffusion coefficient for all species when all $\mathscr{D}_{ij}$ are equal
$\mathscr{D}_{ij}$ = binary diffusion coefficient for species i and j
f = stream function
h = static enthalpy of the gas
$\tilde{h}$ = gas mixture property which reduces to the static enthalpy h when all diffusion coefficients are equal
h° = heat of formation
H_T = total enthalpy
j_k = diffusional mass flux of element k per unit area away from the surface

Received January 6, 1971; revision received March 14, 1972. This work was supported by the Air Force Weapons Lab. under Contract F29601-68-C-0062.

Index categories: Material Ablation; Boundary Layers and Convective Heat Transfer—Turbulent; Reactive Flows.

* Vice President and Manager, Technology Division. Member AIAA.

† Staff Engineer, Technology Division. Member AIAA.

‡ Captain, United States Air Force. Associate Member AIAA.

K = mixing length constant
$\tilde{K}_k$ = total mass fraction of element (or base gas) k irrespective of molecular configuration
l = mixing length
$\dot{m}$ = mass flow rate per unit area
$\mathcal{M}$ = molecular weight of the gas mixture
P = pressure
Pr_t = turbulent Prandtl number
q_a = diffusional heat flux (less viscous work) per unit area away from the surface
q_r = one-dimensional radiant heat flux toward the surface
r = local radius in the boundary layer in a meridian plane
r_o = local radius of body in a meridian plane
s = distance along body from stagnation point or leading edge
$\langle Sc \rangle$ = reference system Schmidt number ($= \rho \bar{D} \mu_2 / \mu_1 M$)
Sc_t = turbulent Schmidt number
t = transverse curvature parameter
T = static temperature
u = velocity component parallel to body surface
v = velocity component normal to body surface
y = distance from surface into the boundary layer, measured normal to the surface
$\tilde{Z}_k$ = a quantity for element (or base species) k which is introduced as a result of the approximation for binary diffusion coefficients and reduces to K_k when all diffusion coefficients are assumed equal (see Ref. 4)
β = streamwise pressure-gradient parameter, $2(\xi/u_1)(du_1/d\xi)$
δ_i^* = incompressible or velocity displacement thickness
$\tilde{\varepsilon}_M$ = $\rho^2 \varepsilon_M / \rho_1 u_1$, normalized turbulent eddy viscosity
η = transformed coordinate normal to the surface
θ = angle between a surface normal and a normal to the body centerline
λ = thermal conductivity
μ = shear viscosity
μ_1, μ_2, μ_3, = properties of the gas mixture (Ref. 4) which reduce to unity, to $\mathcal{M}$ and to $1/\mathcal{M}$, respectively, for assumed equal diffusion coefficients
ν = kinematic viscosity
ξ = transformed streamwise coordinate
ρ = density
$\rho\varepsilon_D$ = average turbulent eddy diffusivity
$\rho\varepsilon_H$ = turbulent eddy conductivity
$\rho\varepsilon_M$ = turbulent eddy viscosity [see Eq. (7)]
τ = local shear stress
ϕ_k = "elemental" source term (see Ref. 4)

Subscripts

c = char
g = gas
i = pertains to the ith species
j = pertains to jth species
k = pertains to kth element (or base species)
w = pertains to wall
1 = reference condition (based on isentropic expansion of reference streamline)

Superscripts

κ = unity for axisymmetric and zero for planar bodies
$'$ = represents partial differentiation with respect to η

I. Introduction

BOUNDARY-LAYER flows over hypersonic vehicles are important to a number of engineering disciplines including vehicle dynamics, heat shield thermodynamics, and vehicle-to-ground communications. For many engineering design and development purposes, relatively simple boundary-layer estimation techniques[1] will suffice for the calculation of drag, heating rates, and shape change of modern re-entry vehicles. The communications engineer, however, is faced with the need for a fairly sophisticated analysis of the vehicle boundary-layer and flowfield before he can even begin to estimate important parameters such as signal attenuation due to electron and ion interference. Restricting our attention to boundary-layer procedures accommodating general equilibrium chemistry and in which ablation products are included in the calculation of chemical species profiles, the laminar flow techniques of Refs. 2–4 are the only codes described in the open literature. The purpose of this paper is to present the extension of the work reported in Ref. 4 to turbulent boundary-layer flows, and to demonstrate the flexibility of the method in difficult analysis situations.

The computational procedure which is described here is suitable for obtaining accurate numerical solutions of the nonsimilar multicomponent laminar and/or turbulent boundary-layer with arbitrary equilibrium chemical systems, unequal diffusion and thermal diffusion coefficients for all species, transverse curvature, and a variety of surface boundary conditions including kinetically controlled or equilibrium solid—gas interface chemistry. For chemically reacting flows, a minimum number of nodes across the boundary-layer is desirable, since a minimum number of chemical state solutions is then required. The solution procedure uses splined quadrics or cubics[4] to represent velocity, enthalpy, and species concentrations between nodes which give smooth variations of the dependent variables and their derivatives through the boundary-layer, therefore allowing significantly fewer nodes for a given accuracy. This advantage is particularly valuable for turbulent boundary-layers, where the very large gradients in the surface-normal direction would require a great number of nodal points for an accurate solution with typical finite difference representations. In the streamwise direction, derivatives are expressed by ordinary implicit difference relations using linear or quadratic curvefits of the dependent variables. The resulting set of algebraic linear and nonlinear simultaneous equations is solved iteratively by the general Newton-Raphson technique.

This paper concentrates on the fluid mechanical aspects of the problem but also describes the basic numerical solution procedure. The procedures employed for calculating the equilibrium state of the gas and the rate-controlled reactions are described elsewhere,[5] as are the calculations of multicomponent transport properties.[6]

Section II of this paper includes the entire mathematical modeling of the boundary-layer flow including discussions of the general conservation equations, turbulent flow considerations, transverse curvature effects, coordinate transformations, and boundary conditions. Section III briefly alludes to the integral matrix method for solving the simultaneous differential equations. Section IV presents some of the results obtained with the program including a few comparisons with data, and Sec. V contains concluding remarks.

II. Mathematical Model of the Boundary Layer

General Conservation Equations

The equations of motion are developed for an axisymmetric or two-dimensional turbulent flow with transverse curvature effects included. The usual turbulent flow technique of breaking the species, velocity, and enthalpy fields into mean and fluctuating components, time averaging, and making appropriate order of magnitude approximations results in the following governing equations, where turbulent transport terms are expressed in Boussinesq form.

Continuity:

$$\partial \rho u r^\kappa / \partial s + \partial \rho v r^\kappa / \partial y = 0 \quad (1)$$

Streamwise Momentum:

$$\rho u(\partial u/\partial s) + \rho v(\partial u/\partial y) = (1/r^\kappa)(\partial/\partial y)[\rho r^\kappa (v + \varepsilon_M)(\partial u/\partial y)] - (\partial P/\partial s) \quad (2)$$

"Elemental" Species:

$$\rho u(\partial \tilde{K}_k/\partial s) + \rho v(\partial \tilde{K}_k/\partial y) = (1/r^\kappa)(\partial/\partial y)[r^\kappa(\rho\varepsilon_D(\partial \tilde{K}_k/\partial y) - j_k)] + \varphi_k \quad (3)$$

Energy:

$$\rho u(\partial H_T/\partial s) + \rho v(\partial H_T/\partial y) = (1/r^\kappa)(\partial/\partial y)[r^\kappa(-q_a + q_r)] \quad (4)$$

The bifurcation approximation for binary diffusion coefficients,[6] i.e., $\mathscr{D}_{ij} = \bar{D}/F_iF_j$, allows explicit formulation of the diffusive flux of "element" k:

$$j_k = -(\rho\bar{D}\mu_2/\mu_1)[\partial\tilde{Z}_k/\partial y + (\tilde{Z}_k - \tilde{K}_k)(\partial\mu_4/\partial y] \quad (5)$$

The term "element" (in quotes) is used to refer to those atoms or groupings of atoms which, according to chemical stoichiometry and equilibrium, are conserved.§ Reference 5 discusses the merits of this approach in detail. The diffusive flux, q_a, of Eq. (4) is defined as

$$q_a = -\left\{\rho(\varepsilon_M + \nu)\frac{\partial(u^2/2)}{\partial y} + (\lambda + \rho\varepsilon_H\bar{C}_p)\frac{\partial T}{\partial y} + \rho\varepsilon_D\left(\frac{\partial h}{\partial y} - \bar{C}_p\frac{\partial T}{\partial y}\right) + \frac{\rho\bar{D}\mu_2}{\mu_1\mathscr{M}}\left[\frac{\partial h}{\partial y} - \left(\tilde{C}_p + \frac{c_t^2R}{\mu_1\mu_2}\right)\frac{\partial T}{\partial y} + c_tRT\frac{\partial\mu_3}{\partial y} + (\tilde{h} - h + c_tRT\mu_3)\frac{\partial\mu_4}{\partial y}\right]\right\} \quad (6)$$

If equal diffusion coefficients are assumed, $\mu_3 = 1/\mathscr{M}$, $\tilde{C}_p = \bar{C}_p$, $\tilde{h} = h$, and when thermal diffusion is to be neglected, $c_t = 0$.

Equations (1–6) comprise the boundary-layer conservation equations, including the approximations for unequal thermal and multicomponent diffusion coefficients. The equations are parabolic in nature, requiring specifications of the dependent variables, their derivatives, or a linear combination thereof along the wall ($y = 0$), edge of the boundary-layer, and at the initial body station. Typical sets of boundary conditions will be discussed later in this paper. Also necessary in the mathematical formulation of the problem is the specification of the molecular transport properties, equation of state and equilibrium (or nonequilibrium) relations for the multicomponent gas, and a description of the eddy viscosity, conductivity, and diffusivity. The molecular transport properties, equation of state, and equilibrium relations are discussed in Refs. 5 and 6. The turbulent flow model is discussed in the next subsection.

Turbulence Model

The boundary-layer flow is divided into a wall region and a wake region. A mixing length formulation for turbulent shear stress was chosen for the wall region, since it appears to offer the most accuracy and flexibility for flows with injection and suction.[7,8] The basic mixing length postulate used in the wall region is

$$\langle(\rho v)'u'\rangle = \rho l^2(du/dy)^2 = \rho\varepsilon_M(du/dy) \quad \text{(wall region)} \quad (7)$$

where l is the mixing length and is related to the scale of turbulence. Prandtl chose to set l equal to Ky, or

$$dl/dy = K, \text{ const} \quad (8)$$

for the low speed flows which he investigated. It has been shown[7] that the Reichardt-Elrod criterion[9,10] will be satisfied if

$$\lim_{y\to 0} l = 0 \quad (9a)$$

$$\lim_{y\to 0}\frac{dl}{dy} = 0 \quad (9b)$$

Assuming that the rate of increase of mixing length is proportional to the difference between the value postulated by Prandtl (Ky) and its actual value results in

$$\frac{dl}{dy} \propto (Ky - l) \quad (10)$$

a relation which satisfies Eq. (9) and asymptotically approaches Eq. (8). The rate of increase of mixing length is assumed to be augmented by the local shear and retarded by the local viscosity. The resulting mixing length differential equation

$$dl/dy = (Ky - l)(\tau/\rho)^{1/2}/y_a^+\nu \quad (11)$$

has been examined in detail for incompressible flows.[7,11] For compressible flows, one can logically derive a similar differential equation by dealing with the mass of an eddy and the total mass available. This results in the mixing length equation

$$\frac{1}{\rho}\frac{d(\rho l)}{dy} = \left(K\int_0^y \rho dy - \rho l\right)\frac{(\tau/\rho)^{1/2}}{y_a^+\mu} \quad (12)$$

which was used in the current analytical procedure. The constants K and y_a^+ have been left unchanged.

In the wake portion of the boundary-layer, a constant eddy viscosity model is used. Clauser's[12] equilibrium boundary-layer expression

$$\varepsilon_M = 0.018\,u_1\delta_1^* \quad \text{(wake region)} \quad (13)$$

was taken as appropriate with the use of the incompressible or kinetic form for the displacement thickness. A satisfactory technique for choosing the correct ε_M expression at any body station is to use the wall region expression, Eq. (7), until ε_M exceeds the wake value, at which point ε_M is held constant at the wake value for the remainder of the boundary-layer thickness. Eddy conductivity and diffusivity are established by the definition of constant turbulent Prandtl and Schmidt numbers:

$$Pr_t = \varepsilon_M/\varepsilon_H, \quad Sc_t = \varepsilon_M/\varepsilon_D \quad (14)$$

A prespecified Reynolds number on momentum thickness, Re_θ, is currently used to trigger transition. Once the transition value for Re_θ is exceeded, turbulent transport properties are immediately brought into the equations of motion. Being a nonsimilar solution, the influence of the upstream laminar profile is felt for some distance downstream. A transition region intermittency model could also be added to the code; however, this change has not been made due to lack of agreement within the boundary-layer community on a realistic model.

Coordinate Transformation

A modified Levy-Lees transformation is used to bring the equations of motion to a more convenient form

$$\eta = \frac{u_1}{\alpha_H(2\xi)^{1/2}}\int_0^y \rho r^\kappa dy \quad (15)$$

$$\xi = \int_0^s \rho_1u_1\mu_1r_0^{2\kappa}ds \quad (16)$$

The modification of the η coordinate by the addition of α_H allows the boundary-layer thickness to be held constant in the solution plane.[4] A stream function f satisfies the global continuity equation automatically:

$$f - f_w = \alpha_H\int_0^\eta \frac{u}{u_1}d\eta \quad (17)$$

$$f_w = -\frac{1}{(2\xi)^{1/2}}\int_0^s \frac{\rho_wv_w}{\rho_1u_1\mu_1r_0^\kappa}d\xi \quad (18)$$

The coordinate transformation then results in the following forms for the streamwise momentum equation*

$$ff'' + \left[\frac{tC(1 + \varepsilon_M/\nu)}{\alpha_H}f''\right]' + \beta\left(\alpha_H^2\frac{\rho_1}{\rho} - f'^2\right) = 2\left(f'\frac{\partial f'}{\partial\ln\xi} - f'^2\frac{\partial\ln\alpha_H}{\partial\ln\xi} - f''\frac{\partial f}{\partial\ln\xi}\right) \quad (19)$$

the energy equation

$$fH_t' + [t(-q_a^* + q_r^*)]' = 2\left(f'\frac{\partial H_t}{\partial\ln\xi} - H_t'\frac{\partial f}{\partial\ln\xi}\right) \quad (20)$$

and the "elemental" species equation

$$f\tilde{K}_k' + \left[t\left(\frac{\tilde{\varepsilon}_M}{\alpha_HSc_t}\tilde{K}_k' - j_k^*\right)\right]' + \alpha_H\phi_k = 2\left(f'\frac{\partial\tilde{K}_k}{\partial\ln\xi} - \tilde{K}_k'\frac{\partial f}{\partial\ln\xi}\right) \quad (21)$$

§ Equal in number to the number of molecular species less the number of independent equilibrium relations.

* It should be noted that the reference conditions (ρ_1, u_1, etc.) are based on the isentropic expansion of a reference streamline to the local pressure and are not necessarily representative of the edge state. This maintains the validity of the Bernoulli relation between the pressure and reference velocity gradients implied by the introduction of β.

where the normalized diffusive energy flux becomes

$$q_a^* = -\frac{C}{\alpha_H}\left\{\frac{f'f''}{\alpha_H^2}u_1^2 + \frac{\bar{C}_p}{Pr}T' + \frac{1}{\langle Sc\rangle}\left[\tilde{h}' - \left(\tilde{C}_p + \frac{c_t^2 R}{\mu_1\mu_2}\right)T' + c_t RT\mu_3' + (\tilde{h} - h + c_t RT\mu_3)(ln\mu_2 T^{c_t})'\right]\right\} - \frac{\tilde{\varepsilon}_M}{\alpha_H}\left[\frac{f'f''}{\alpha_H^2}u_1^2 + \frac{\bar{C}_p}{Pr_t}T' + \frac{1}{Sc_t}(h' - \bar{C}_p T')\right] \quad (22)$$

and the normalized molecular diffusive flux of the kth "elemental" species is

$$j_k^* = -(C/\alpha_H\langle Sc\rangle)[\tilde{Z}_k' + (\tilde{Z}_k - \tilde{K}_k)\mu_4'] \quad (23)$$

In these equations the transverse curvature effect is included entirely in the coordinate transformation and in the definition of t†

$$t \equiv \left(\frac{r}{r_0}\right)^2 = 1 + \frac{2\alpha_H(2\xi)^{1/2}\cos\theta}{u_1 r_0^2}\int_0^\eta \frac{1}{\rho}d\eta \quad (24)$$

The turbulent model equations are transformed in a similar fashion.

Boundary Conditions

The usual set of boundary conditions for the boundary-layer flow problem consists of the specification of initial profiles for the dependent variables f', H_T, and $\tilde{K}_k$, plus additional specifications of these quantities along the wall and at the edge of the boundary-layer, and the specification of f_w along the wall. However, since the main utilization for the technique presented here is to compute boundary-layer properties for flows over ablating or transpired surfaces (heat shields, rocket nozzles, etc.), these boundary conditions have been greatly generalized. The numerous options resulting from this generalization are discussed below.

Boundary-layer edge conditions may be found by several techniques. For analyses of the region near a stagnation point, the specification of the stagnation pressure and enthalpy and the generation of an isentropic expansion to prespecified edge pressures is often satisfactory. The technique which is most useful for analyses of long re-entry bodies consists of prespecifying entropy as a function of stream function. The program then determines its own correct boundary-layer edge condition based on the latest interated value for the stream function at the boundary-layer edge. The isentropic expansion option will be demonstrated in a sample problem presented later in this paper.

Initial profiles of f', H_T, and $\tilde{K}_k$ are most difficult to establish for the general problem; therefore, calculations are often started with reasonable assumed profiles far upstream of the region of interest so that effects of these assumptions will die out. Another possibility for initially laminar problems is to assume a similar solution as a starting profile. This assumption reduces the equations to ordinary differential equations at the starting point, which may be solved simultaneously for a set of profiles unique to the assumed edge and wall state. The initially similar solution is exact at a body stagnation point; therefore, this option is particularly valuable for blunt body problems.

Practical boundary-layer problems involving ablation or transpiration demand a broad range of surface boundary conditions specifications. These may include (in addition to the no-slip velocity constraint, $f_w' = 0$) a) assigned mass fluxes of transpired or ablated components; b) surface equilibrium between a surface and the adjacent gases; c) kinetically controlled surface mass removal based on the composition of the gas phase species at the wall; d) quasi-steady energy balances at the surface; e) assigned surface temperature; f) assigned surface energy accommodation.

Any physically valid combination of these specifications can be accommodated by the program. For example, the transpired coolant rate required to maintain a nonablating surface at a specified temperature uses conditions d and e. Quasi-steady equilibrium ablation solutions use b and d; adiabatic, impermeable, nonreacting wall solutions use a, zero flux, and f. The adaptability of the program to this range of boundary conditions has permitted its use for a number of fundamental studies,[14,15] as well as the evaluation of a range of thermal protection concepts.

† This contrasts to Ref. 13 where t is defined as $(r/r_0)^2 - 1$.

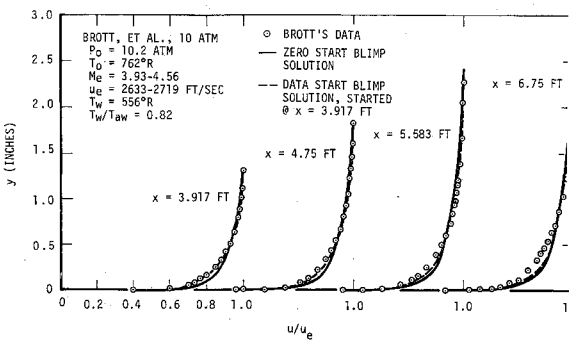

Fig. 1 Velocity ratio profiles for hypersonic, negative pressure gradient flow.

III. Solution Procedure

The equations of motion are solved by a technique which can be classified as an integral strip method, since the governing partial differential equations are integrated across boundary-layer strips. This technique has been presented in detail in Ref. 4; therefore, it will be reviewed only briefly here.

The equations are transformed to ordinary differential equations by the introduction of implicit, finite difference expressions for the streamwise derivatives. The ordinary differential equations are transformed to algebraic form by defining boundary-layer strips (or nodes), sampling the dependent variables and their derivatives only at these nodes, and writing Taylor series equations relating these dependent variables to their derivatives. Rather than use finite difference expressions, however, a cubic polynomial for the primary variable is assumed between each pair of nodes, thus allowing the Taylor series equations to be truncated appropriately. The final step in the treatment of the conservation equations is their integration across the boundary-layer strips. The primary reason for this integration is to simplify the η-derivative terms in the energy and species conservation equations, since it is not convenient to express the complex q_a^* and j_k^* terms in any other form. The set of simultaneous algebraic equations, which now includes the Taylor series, the conservation equations, and the boundary conditions, is solved by general Newton-Raphson iteration. Typically, 3 to 6 iterations are required to reach a satisfactory solution at each body station, at approximately one second per iteration on modern computers.

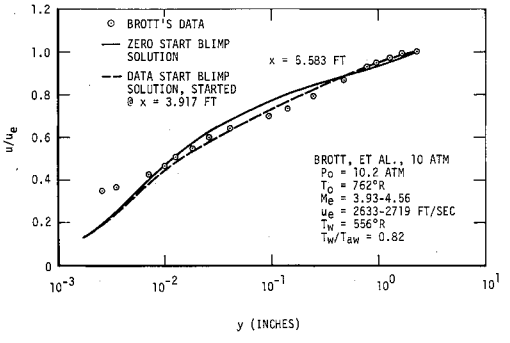

Fig. 2 Linear-log velocity ratio profiles for hypersonic, negative pressure gradient flow.

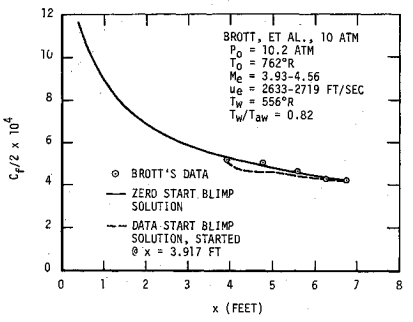

Fig. 3 Skin-friction coefficient for hypersonic, negative pressure gradient flow.

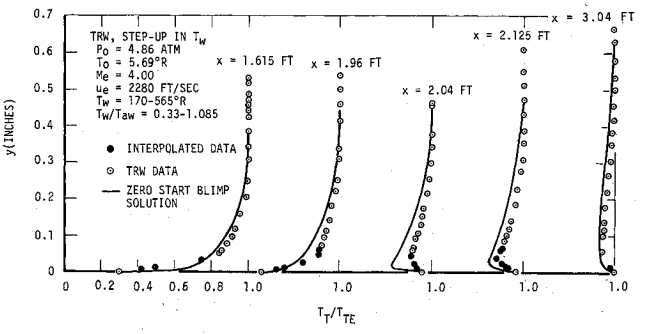

Fig. 5 Total temperature ratio profiles for flow with step-up in wall temperature.

IV. Sample Problems

The success of this flow model and computer solution technique for incompressible flow problems is well documented.[7,11] In the present paper, sample problems were selected to demonstrate the accuracy of the solution technique for compressible flows and to demonstrate the use of the technique in ablation problems.

Accelerating Nozzle Flow Case

The experimental investigations of Brott et al.[16] were performed in the Naval Ordnance Lab. Mach 5 boundary-layer channel, which is a two-dimensional half nozzle with a flexible wall forming the nozzle. Boundary-layer measurements were made on the opposite, flat wall with moderate heat transfer to the wall controlled by circulating wall coolant. Instrumentation used in these tests included total and static pressure probes, equilibrium (recovery) temperature probe, thermocouple probe, skin friction balances, and wall heat flux gages.

Two different all-turbulent flow predictions were prepared for the Brott data. One of these, the "zero start" solution, was started with an assumed profile at the nozzle throat ($x = 0$), and made use of the reported pressure distribution along the entire nozzle. The other (data start) solution used the reported experimental data profiles at $x = 47$ in. as initial profiles and marched on from there. The results are shown in Figs. 1–3. Figure 1 presents predicted velocity profiles and experimental data at four stations along the nozzle. The zero start and data start profile predictions are seen to approach one another in shape by the last data station. Both forms of prediction tend to overpredict velocity by as much as 15% up to velocity ratios of 0.9, then underpredict in the far wake region. This can be seen more clearly in the logarithmic plot of Fig. 2. The data points very near the wall are thought to be incorrect due to wall interference and low probe Reynolds number effects. Figure 3 indicates the drag coefficient data and prediction agreement, which is seen to be very good. The wiggle in the data start curve is due to adjustments from the input data profile.

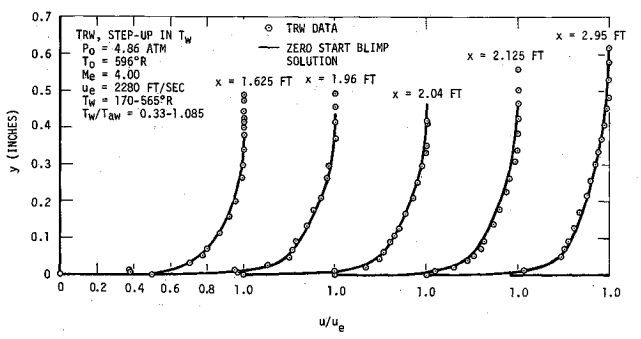

Fig. 4 Velocity ratio profiles for flow with step-up in wall temperature.

Step in Wall Temperature Case

Recent experiments,[17,18] run at AEDC Supersonic Wind Tunnel "A" under the direction of TRW Systems Group personnel, form the basis for the next comparisons. The test model was a 20-in. i.d., 49.5 in. long hollow cylinder aligned with the flow. A 400°F step in wall temperature was made between the 23.0 and 24.0 in. stations by changing the wall coolant from liquid nitrogen to water at this point. Instrumentation for these tests included total and static pressure probes, stagnation temperature probe,

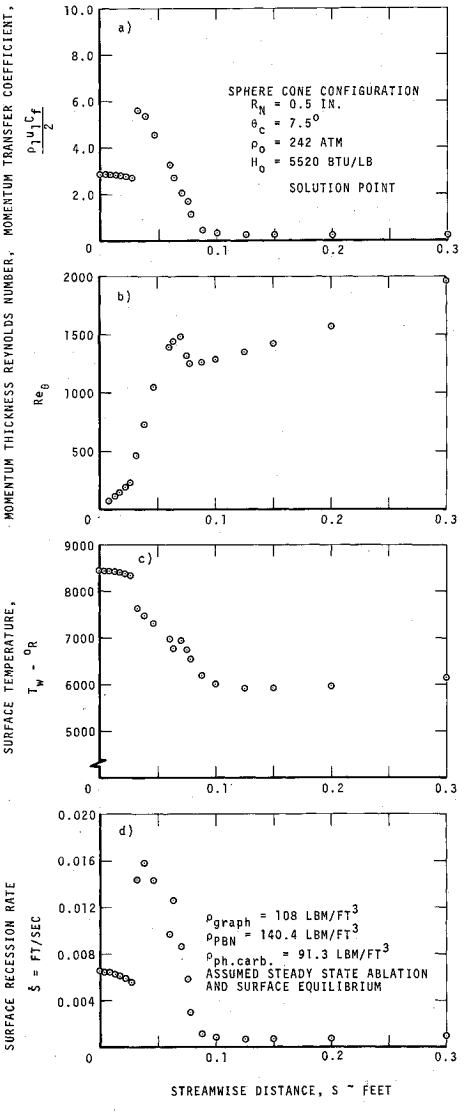

Fig. 6 Calculated distributions of a) momentum transfer coefficient, b) momentum thickness Reynolds number, c) surface temperature and d) surface recession rate.

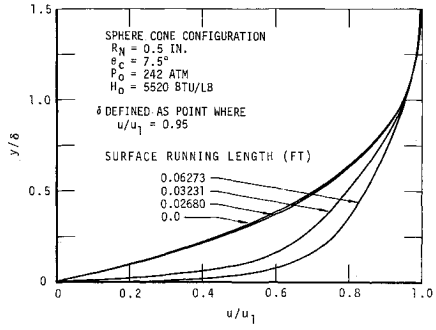

Fig. 7 Velocity profiles at several stations.

hot wire anemometer, surface temperature thermocouples, Gardon heat transfer gages, and Stanton tubes. These experiments were selected as a good sample problem since they illustrate the relaxation of the thermal boundary-layer downstream of the temperature step in a Mach 4 flow.

Velocity and total temperature profiles are shown in Figs. 4 and 5. Velocity prediction is much improved for this case. Of particular interest is the prediction of temperature in the vicinity of the wall temperature jump. Included in Fig. 5 are shaded data points, reported in Ref. 18, which represent interpolated data and must be treated as approximate. Based upon the actual measured data (open symbols), the prediction technique does a good job of describing the response of the boundary-layer to a jump in wall temperature.

Sphere-Cone Configuration with Laminar and Turbulent Flow

A final sample problem was selected which demonstrates the use of the program as an ablation prediction tool and also includes flow transition from a laminar to a turbulent state. No experimental profile data are included, since none are available for graphite ablation problems. The configuration chosen was a 0.500-in. nose radius, 7.5° half angle sphere-cone consisting of three surface materials: graphite, pyrolytic boron nitride, and phenolic carbon. Graphite was the surface material from $s = 0$ to 0.0268 ft, then boron nitride to $s = 0.0600$ ft, with phenolic carbon over the remainder of the surface. Stagnation conditions were representative of a single time in a severe re-entry trajectory with $P_o = 242$ atm, $H_o = 5520$ Btu/lb. A total surface running length of 5.0164 ft was analyzed in this problem, which required 29 body stations and thirteen nodes through the boundary-layer. For this sample problem, the option of a quasi-steady energy balance at the wall was used, in addition to demanding surface chemical equilibrium, for all three surface materials. The program then calculates its own ablation rate, wall species concentrations, and temperature levels based on the energy balance and chemical equilibrium requirements.

The calculation was started at the stagnation point and an isentropic expansion was assumed. The flow was allowed to transist at $Re_\theta = 250$. Figure 6a illustrates the distribution of $C_f/2$ over the first 0.30 ft of surface running length. As can be seen in the $C_f/2$ distribution, transition occurred between $S = 0.0268$ and $S = 0.0323$ ft. The distribution of Reynolds number on momentum thickness may be seen in Fig. 6b. Figure 6c illustrates the wall temperature distribution that results from the steady state energy balance and surface equilibrium assumption, and Fig. 6d illustrates the calculated quasi-steady surface recession rate.

Profile information for this problem is particularly interesting since both boundary-layer-transition and surface-material changes occur over the forward portion of the body. Velocity profiles are presented in Fig. 7. The body stations selected include the stagnation point (0.0 ft), flow just ahead of transition (0.02681 ft), flow just after transition which happens to be over the boron nitride just past the C-BN discontinuity (0.03231 ft), and flow over the phenolic carbon just past the BN-phenolic carbon discontinuity (0.06273 ft). The first two profiles are clearly laminar in nature, whereas the third is more transitional. The last profile appears to have the shape of a fully turbulent flow. This gradual evolution of a turbulent shape occurs because the turbulent transport terms in the equations of motion are small in the vicinity of the transition point. Species concentration profiles for the same four stations are presented in Figs. 8a–8d. It is interesting to observe that the region of greatest chemical interaction appears to shrink further and further away from the outer edge of the boundary-layer as the flow progresses downstream. This is consistent with the knowledge that the laminar sublayer grows at a slower rate than the turbulent core flow. Another interesting feature of these species profiles is shown in Fig. 8d, where it can be seen that a significant mole fraction of boron compounds persists in the boundary-layer, although the flow is adjacent to a phenolic carbon surface at that station. A total of 60 species was considered in this problem, but only those exhibiting a mole fraction greater than 0.001 somewhere in the boundary-layer are shown graphically.

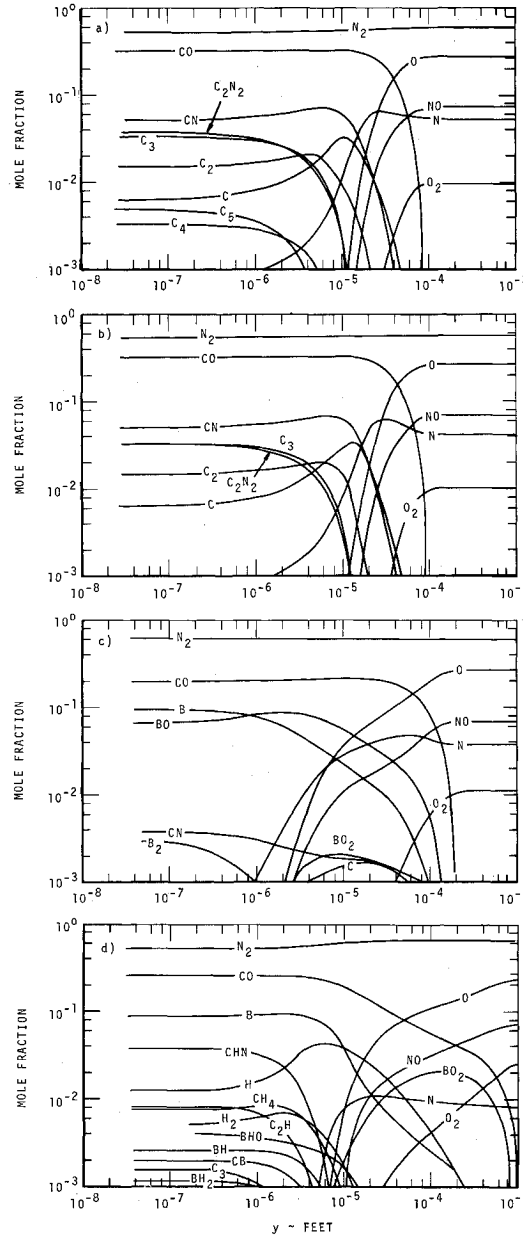

Fig. 8 Species concentration profiles at *a*) $S = 0.0$ ft, *b*) $S = 0.0268$ ft, *c*) $S = 0.0321$ ft, and *d*) $S = 0.0673$ ft.

V. Conclusions

The purpose of this paper has been to present a sophisticated analysis technique for laminar or turbulent multicomponent boundary-layer flows with difficult boundary conditions, generally resulting from ablation or transpiration at the boundary. The numerical solution procedure includes physically realistic combinations of wall boundary conditions, including equilibrium or nonequilibrium heterogeneous chemical reactions and energy balances at the wall. Boundary-layer edge conditions permit precise inclusion of entropy-layer effects. In its present formulation, the program is ideally suited for the engineer who needs detailed boundary-layer information for a variety of wall-material—fluid combinations. The code has also proved to be very valuable in developing engineering correlations suitable for design and tradeoff studies.[15] The compressible turbulent model within the code is an adaption of a previously verified incompressible model. Comparisons with compressible flow data support this model and the three original (and invariant) model constants.

References

[1] Schurmann, E. E. H., "Engineering Methods for the Analysis of Aerodynamic Heating," RAD-TM-63-68, Nov. 1963, Avco Corp., Wilmington, Mass.

[2] Luceri, J. A., "Re-entry Environment and Systems Technology (REST) Semiannual Progress Report, 1 Jan.–30 June 1966, Volume II —Aerophysics Appendices," Rept. AVMSD-0207-66-CR, Vol. II, July 1966, Avco Corp., Wilmington, Mass.

[3] Lew, H. G., "The Ionized Flow Field Over Re-entry Bodies," Rept T.I.S. R67SD70, Dec. 1967, General Electric, Missile and Space Div., King of Prussia, Pa.

[4] Kendall, R. M. and Bartlett, E. P., "Nonsimilar Solution of the Multicomponent Laminar Boundary Layer by an Integral Matrix Method," *AIAA Journal*, Vol. 6, No. 6, June 1968, pp. 1089–1097.

[5] Kendall, R. M., "A General Approach to the Thermochemical Solution of Mixed Equilibrium-Nonequilibrium, Homogeneous or Heterogeneous Systems," CR-1064, June 1968, NASA.

[6] Kendall, R. M., Rindal, R. A., and Bartlett, E. P., "A Multicomponent Boundary Layer Chemically Coupled to an Ablating Surface," *AIAA Journal*, Vol. 5, No. 6, June 1967, pp. 1063–1071.

[7] Kendall, R. M., Rubesin, M. W., Dahm, T. J., and Mendenhall, M. R., "Mass, Momentum, and Heat Transfer Within a Turbulent Boundary Layer with Foreign Gas Mass Transfer at the Surface, Part I—Constant Fluid Properties," AD 619209, Rept. 111, Feb. 1964, Vidya Division, Itek Corp, Palo Alto, Calif.

[8] Squire, L. C., "A Law of the Wall for Compressible Turbulent Boundary Layers with Air Injection," *Journal of Fluid Mechanics*, Vol. 37, Part 3, July 1969, pp. 449–456.

[9] Reichardt, H., "Complete Representation of the Turbulent Velocity Distribution in Smooth Pipe," *Zeitschrift für Angewandte Mathematik und Mechanik*, Vol. 32, No. 7, July 1951, pp. 208–219.

[10] Elrod, H. G., "Note on the Turbulent Shear Stress Near a Wall," *Journal of the Aeronautical Sciences*, Vol. 24, No. 6, June 1957, pp.

[11] Kendall, R. M. and Anderson, L. W., "Nonsimilar Solution of the Incompressible Turbulent Boundary Layer," *Proceedings of the 1968 AFOSR-IFP-Stanford Conference on Computation of Turbulent Boundary Layers*, edited by S. J. Kline et al., Stanford Univ., Mechanical Engineering Rept., Stanford, Calif., Aug. 1968, pp. 366–374.

[12] Clauser, F. H., "The Turbulent Boundary Layer," *Advances in Applied Mechanics*, Vol. IV, Academic Press, New York, 1956, pp. 1–51.

[13] Jaffe, N. A., Lind, R. C., and Smith, A. M. O., "Solution to the Binary Diffusion Laminar Boundary Layer Equations with Second Order Transverse Curvature," *AIAA Journal*, Vol. 5, No. 9, Sept. 1967, pp. 1563–1569.

[14] Wolfram, W. R. and Walker, W. F., "The Effects of Upstream Mass Injection on Downstream Heat Transfer," *Transactions of the ASME: Journal of Heat Transfer*, Vol. 92, No. 3, Aug. 1970, pp. 385–392.

[15] Putz, K. E. and Bartlett, E. P., "Heat Transfer and Ablation-Rate Correlations for Re-entry Heat-Shield and Nosetip Applications," Paper 72-91 at the AIAA 10th Aerospace Sciences Meeting, San Diego, Calif., Jan. 17–19, 1972.

[16] Brott, D. L., Yanta, W. J., Voisinet, R. L., and Lee, R. E., "An Experimental Investigation of the Compressible Turbulent Boundary Layer with a Favorable Pressure Gradient," Rept. NOLTR 69-143, Aug. 25, 1969, Naval Ordnance Lab., White Oak, Md.

[17] Unpublished test data received from J. E. Lewis, TRW Systems, Redondo Beach, Calif. Data groups 61-77, 134-157, and 200-244 of Project No. VA0084, SAMSO-TRW Turbulent Boundary Layer Study completed Aug. 26, 1970.

[18] Hahn, J. S. and Lutz, R. G., "Experimental Investigation of Turbulent Boundary Layers with Pressure Gradient and Heat Transfer at Mach Number 4," AEDC-TR-71-3, Jan. 1971, von Karman Gas Dynamics Facility, Air Force Systems Command, Arnold Air Force Station, Tenn.